AGU PUBLICATIONS

Geophysical Research Letters

RESEARCH LETTER
10.1002/2015GL066344

Key Points:
- The climate system switched from a bistable to monostable state around 30 ka
- Early warning signals of this bifurcation are detected in δ^{18}O ice core data
- Low obliquity caused greatly expanded sea ice in the Labrador Sea

Supporting Information:
- Supporting Information S1
- Movie S1

Correspondence to:
C. S. M. Turney,
c.turney@unsw.edu.au

Citation:
Turney, C. S. M., et al. (2015), Obliquity-driven expansion of North Atlantic sea ice during the last glacial, *Geophys. Res. Lett.*, *42*, 10,382–10,390, doi:10.1002/2015GL066344.

Received 7 OCT 2015
Accepted 17 NOV 2015
Accepted article online 24 NOV 2015
Published online 10 DEC 2015

Obliquity-driven expansion of North Atlantic sea ice during the last glacial

Chris S. M. Turney[1], Zoë A. Thomas[1], David K. Hutchinson[1,2], Corey J. A. Bradshaw[3], Barry W. Brook[4], Matthew H. England[1,2], Christopher J. Fogwill[1], Richard T. Jones[5], Jonathan Palmer[1], Konrad A. Hughen[6], and Alan Cooper[7]

[1]Climate Change Research Centre, School of Biological, Earth, and Environmental Sciences, University of New South Wales, Sydney, New South Wales, Australia, [2]ARC Centre of Excellence for Climate Systems Science, University of New South Wales, Sydney, New South Wales, Australia, [3]School of Biological Sciences and The Environment Institute, University of Adelaide, Adelaide, South Australia, Australia, [4]School of Biological Sciences, University of Tasmania, Hobart, Tasmania, Australia, [5]Geography, Exeter University, Devon, UK, [6]Department of Marine Chemistry and Geochemistry, Woods Hole Oceanographic Institution, Woods Hole, Massachusetts, USA, [7]Australian Centre for Ancient DNA, School of Biological Sciences and The Environment Institute, University of Adelaide, Adelaide, South Australia, Australia

Abstract North Atlantic late Pleistocene climate (60,000 to 11,650 years ago) was characterized by abrupt and extreme millennial duration oscillations known as Dansgaard-Oeschger (D-O) events. However, during the Last Glacial Maximum (LGM) 23,000 to 19,000 cal years ago (23 to 19 ka), no D-O events are observed in the Greenland ice cores. Our new analysis of the Greenland δ^{18}O record reveals a switch in the stability of the climate system around 30 ka, suggesting that a critical threshold was passed. Climate system modeling suggests that low axial obliquity at this time caused vastly expanded sea ice in the Labrador Sea, shifting Northern Hemisphere westerly winds south and reducing the strength of meridional overturning circulation. The results suggest that these feedbacks tipped the climate system into full glacial conditions, leading to maximum continental ice growth during the LGM.

1. Introduction

The Last Glacial Maximum (LGM) from 23,000 to 19,000 cal years ago (23 to 19 ka) is associated with a summer insolation minimum at 65°N, but understanding how this period of maximum ice volume was synchronized globally remains unclear [*European Project for Ice Coring in Antarctica Community Members*, 2006; *He et al*., 2013; *Mix et al*., 2001; *Vandergoes et al*., 2005]. Potentially important in this regard are Dansgaard-Oeschger (D-O) events, millennial-scale climate oscillations that switched the northern climate rapidly and temporarily from relatively cold to warm atmospheric conditions (up to Δ16°C), which are bundled into decreasing amplitude cooling cycles culminating in massive discharges of ice into the North Atlantic (Heinrich or H events) [*Bond et al*., 1993; *Wolff et al*., 2010]. D-O events are most strongly expressed in the Greenland ice cores during the period of 60–30 ka, followed by some 16 kyr (thousand years) of relatively stable cold conditions before the late glacial interstadial warming (the Bølling-Allerød or GI-1; 14.6 ka) and subsequent Younger Dryas stadial (GS-1) [*Bond et al*., 1993; *Masson-Delmotte et al*., 2005; *Wolff et al*., 2010; *Rasmussen et al*., 2014] (Figure 1). The cessation of millennial duration D-O events after 30 ka parallels a shift to excess deuterium isotope values in the Greenland Ice Core Project record, which has been interpreted to result from greater sea ice extent and a stronger penetration of southern (warmer) Atlantic-sourced precipitation prior to and during the LGM [*Masson-Delmotte et al*., 2005]. The changing timing and amplitude of D-O events might therefore offer important insights into the trigger(s) and feedback governing the onset and structure of the LGM.

The distinctive shape of late Pleistocene D-O events in Greenland (Figure 1) implies rapid and extreme changes in the North Atlantic wind field [*Wunsch*, 2003] and demonstrates the presence of multistability in the climate system that might have relevance over longer time scales [*Maslin and Brierley*, 2015; *Paillard*, 1998]. Others have reported a bifurcation in the GICC05 δ^{18}O record, implying that the climate system shifted from a bistable to a monostable state sometime prior to the LGM [*Livina et al*., 2010]. The precise timing, mechanism(s), and wider ramifications of this change remain unresolved, however, limiting our understanding of high-frequency climatic variability within the Earth's system.

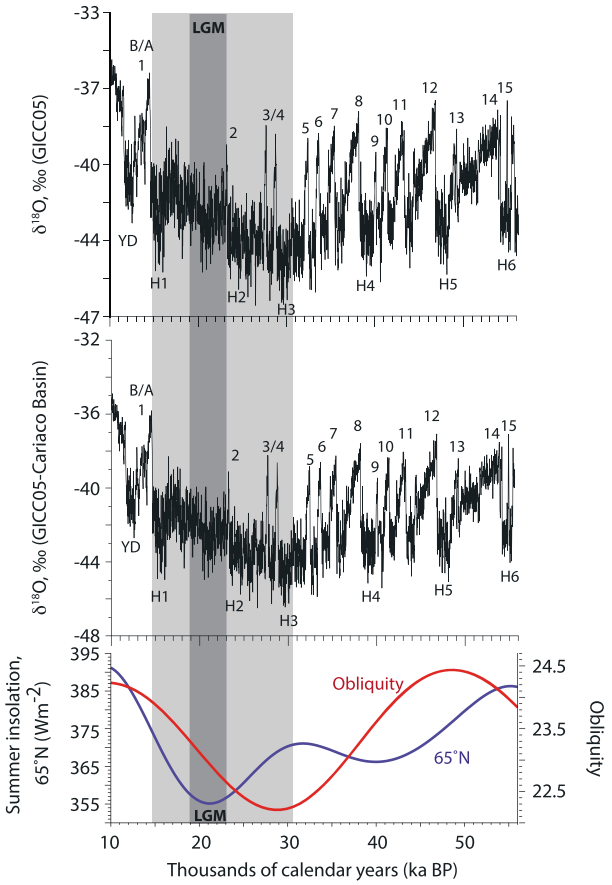

Figure 1. The Greenland ice core δ^{18}O record top panel GICC05 and middle panel combined GICC05-CB chronology) and changing obliquity and 65°N summer insolation (bottom panel). Limited Dansgaard-Oeschger expression is defined by the light grey column and the Last Glacial Maximum (LGM) by the dark grey column. Numbers denote Dansgaard-Oeschger (D-O)/Greenland interstadial (GI) events as recognized in the ice core record. Heinrich events are given by "H1-6."

2. Detecting a Tipping Point

To explore the timing of this bifurcation, we used the GICC05 δ^{18}O record to reconstruct the shape of the state space of the system through the modality of the distribution, by estimating the inverted empirical probability density of the data over different sliding windows (see Text S1 in the supporting information). This method is based on the interpretation of the dynamics of the climate system as randomly forced motions in a one-dimensional potential landscape based on the stationary probability distribution of a stochastic system [*Livina et al.*, 2010]. While chaotic and nonstationary dynamics have been proposed as alternative mechanisms [*Timmermann et al.*, 2003], the above framework is appropriate in this context because recent analysis of the individual D-O events suggests that they are triggered purely by stochastic noise, with no evidence of underlying periodicity [*Ditlevsen and Johnsen*, 2010; *Schulz*, 2002]. Since the mean recurrence time of D-O events is 2.8 kyr [*Ditlevsen et al.*, 2007], a sliding window of 10 kyr has the lowest probability of erroneous detection of the number of states present [*Livina et al.*, 2011]. We thus used this sliding window size to generate a series of inverted empirical probability density histograms over time (Figure 2 and Movie S1 in the supporting information).

Changes in the number of states represent bifurcations in the system [*Livina et al.*, 2010, 2011]. On the approach to a bifurcation, or "tipping point," a phenomenon called "critical slowing down" is often observed. Here the basin of attraction of the system starts to become wider and shallower [*van Nes and Scheffer*, 2007]. Consequently, if the system is perturbed slightly, it will travel farther in the basin of attraction and take longer to return to its stable state. The system thus becomes increasingly slow in recovering from minor perturbations. Early warning signals of approaching tipping points can be identified by analyzing the pattern of fluctuations in the short-term trends of a time series preceding the transition; the increased recovery time is detected as a short-term increase in the autocorrelation or "memory" of the time series [*Ives*, 1995]. An increasing trend in variance is also often found due to the ability of the system to travel farther from its equilibrium point as the basin of attraction shallows and widens.

We therefore used the GICC05 δ^{18}O record to investigate whether we could detect early warning signals of this bifurcation (Figure 3). We preprocessed the data by applying a Gaussian kernel smoothing function over a bandwidth sufficient to remove long-term trends; this is necessary due to nonstationarities in paleoclimate data. We chose a smoothing bandwidth such that the long-term trends are removed but the data are not overfitted [*Dakos et al.*, 2008]. We then obtained the residual time series by subtracting the smoothed record from the original record. We then measured autocorrelation at lag 1 and variance within a sliding window of analysis (50% of data length) [*Dakos et al.*, 2008]. A sensitivity analysis was undertaken to ensure that the results are robust over a range of smoothing bandwidths and sliding window sizes. We applied the

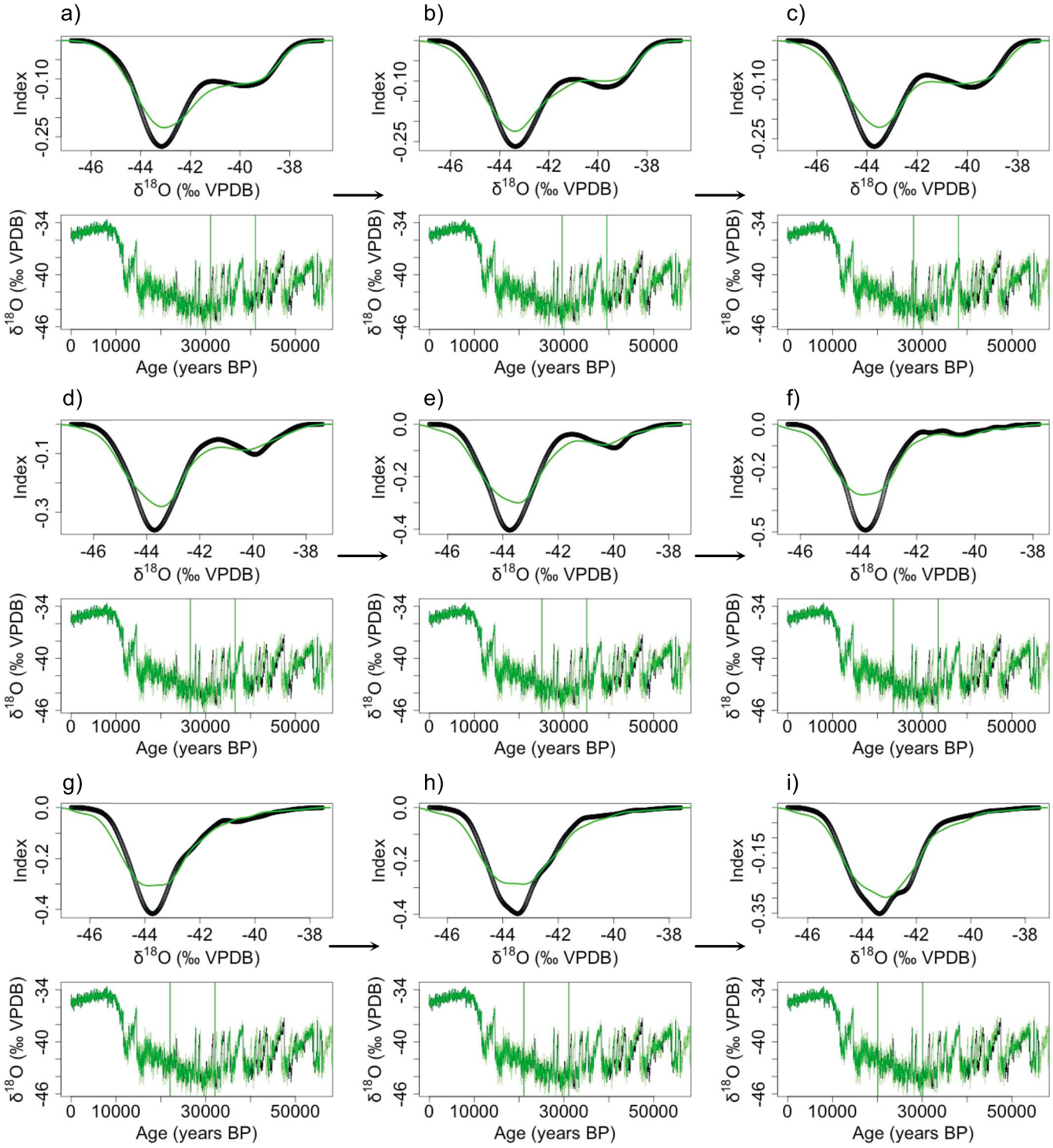

Figure 2. (a–i) Nine time slices showing the changing shape of the potential well over time using the GICC05 time scale (green) and the alternative GICC05-CB time scale (black), capturing the transition from a bistable to a monostable state over the period of 35–20 ka. The vertical green lines indicate the size of the sliding window of analysis. See Movie S1 in the supporting information for the full record.

nonparametric Kendall's τ rank correlation coefficient to measure the trends in autocorrelation and variance by assessing the predominance of concordant pairs, providing an objective evaluation of the statistical evidence for the trend [*Kendall*, 1948]; this was measured from 40 ka associated with the 65°N minimum in summer insolation (Figure 1). To test whether these results are statistically different from random, we created

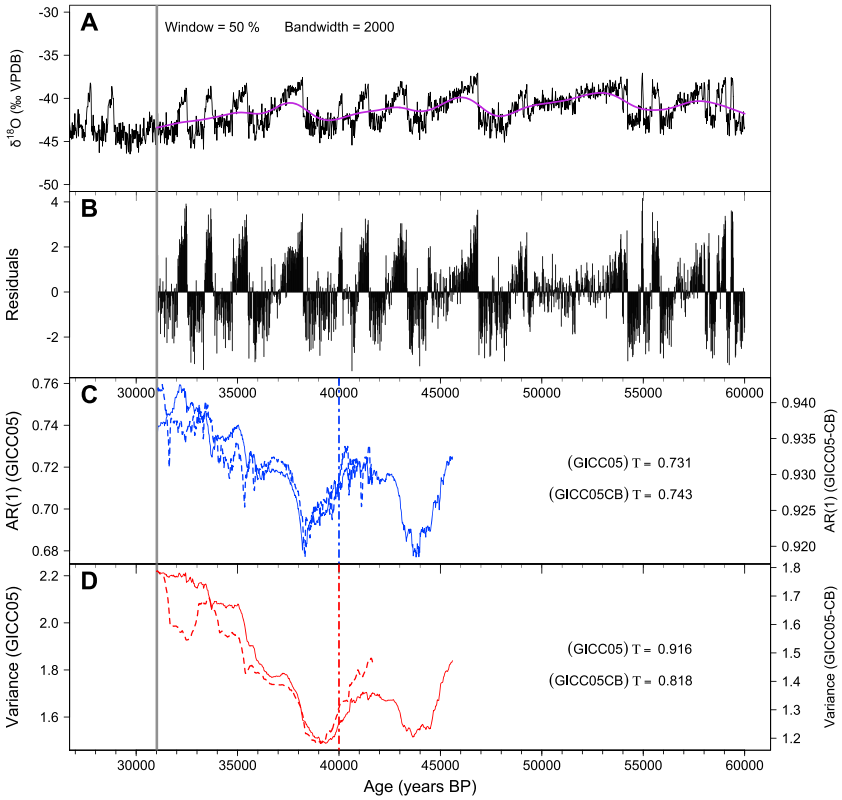

Figure 3. Time series analysis of Greenland δ^{18}O on the GICC05 and GICC05-CB chronology from 60 ka to 31 ka. (a) Greenland δ^{18}O (GICC05) with Gaussian-kernel-smoothing filter shown (purple line). (b) Residuals from the detrended data. (c) Autocorrelation over the sliding window (window = 50% of data) GICC05 (solid blue line) and GICC05-CB (dashed blue line). (d) Variance over the sliding window with GICC05 (solid red line) and GICC05-CB (dashed red line). Kendall's τ indicate the statistical evidence for the trend, calculated from 40 to 31 ka (blue and red dashed lines in Figures 3c and 3d).

a surrogate data set by randomizing the original data over several thousand permutations (Text S1 in the supporting information). The probability of making a type I statistical error for the original data is obtained by comparing to the probability distribution of the surrogate data. This randomization method guarantees the same amplitude distribution as the original time series but removes any ordered structure or linear correlation [*Theiler et al.*, 1992]. Autocorrelation and variance were computed for the surrogate time series, and a histogram constructed to show the frequency distribution of the trend statistic (in this case, Kendall's τ). We used the 90th and 95th percentiles to provide the 90% and 95% rejection thresholds, respectively (Figure 4). If the value computed for the original time series lies beyond the thresholds created by the surrogate time series, we can reject the null hypothesis (i.e., no nonrandom trend) and calculate the probability of making a type I error [*Theiler et al.*, 1992].

3. Exploring an Alternative Greenland Chronology

Previous studies have demonstrated that the spectral characteristics in Greenland ice core records depend on the chronology used [*Ditlevsen et al.*, 2007], and multicentennial corrections have been identified in GICC05 [*Svensson et al.*, 2008; *Rasmussen et al.*, 2014; *Buizert et al.*, 2015; *West Antarctic Ice Sheet* (*WAIS*) *Divide Project Members*, 2015], suggesting that refinements in age modelling could offer new insights into past climate dynamics while also testing the robustness of analyses. Using known relationships between Northern Hemisphere temperatures and associated changes in tropical rainfall belts [*Hughen et al.*, 1996; *Overpeck et al.*, 1989; *Rind*, 1998; *Rind et al.*, 2001; *WAIS Divide Project Members*, 2015], an alternative Greenland ice core chronology for the onset of abrupt warming events has been developed in combination with the independently -dated Cariaco Basin marine sedimentary sequence (constrained by Hulu Cave U-Th ages); with the latter preserving a record of millennial-scale changes in the Atlantic Intertropical Convergence Zone [*Cooper et al.*, 2015; *Deplazes et al.*, 2013;

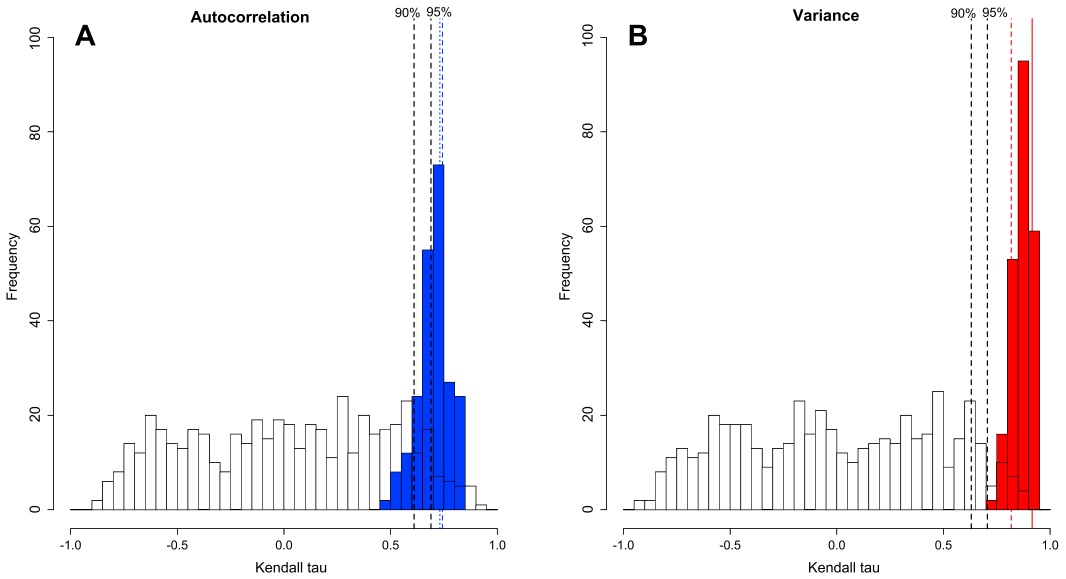

Figure 4. These graphs illustrate the results of both the statistical analysis and the sensitivity analyses. The black histograms show the frequency distribution of Kendall τ from 1000 realizations of the surrogate time series model. The black dashed lines indicate the 90 and 95% rejection thresholds. The blue/red histograms overlaid show the distribution of Kendall τ over a range of sliding window sizes and smoothing bandwidths for autocorrelation and variance, respectively. The type 1 error probability falls <0.05 for all realizations of the sensitivity analysis for variance, and most fall <0.01 for the sensitivity analysis for autocorrelation. The solid (dashed) blue line shows the Kendall τ value from the GICC05 (GICC05-CB) time series for autocorrelation, and the solid (dashed) red line shows the Kendall τ from the GICC05 (GICC05-CB) time series for variance, for the window size of 50% and bandwidth of 2000, as used in Figure 3.

Hughen et al., 2006; *Peterson et al.*, 2000; *Tzedakis et al.*, 2007] (Text S2 in the supporting information). By deriving an alternative replicated framework for the Greenland ice core chronology in (that fits within the uncertainty of both timescales) parallel to GICC05, we tested for and identified the drivers of limited D-O expression in the North Atlantic over the period of 30 to 14.6 ka. We then resampled the resulting record (henceforth "GICC05-CB") at the same 20 year resolution as GICC05 (Figure 1). While the GICC05-CB has the same $\delta^{18}O$ structure, the alternative chronology allows us to test the robustness of the time series analyses generated from GICC05.

4. Results and Discussion

Results of our stability analysis (Figure 2) show a switch from a bistable to a monostable state due to the loss of stability of the warm interstadial state, consistent with previous studies [*Livina et al.*, 2010]. Since the timing of the bifurcation is inherently dependent on the size of the sliding window of analysis, our sensitivity analysis used sliding window sizes from 5 to 15 kyr to investigate the effect of this parameter on the timing of the bifurcation. We found that with window sizes >6 kyr, the monostable state is present around 30 ka (Figure S1 in the supporting information), 5000 years earlier than previously reported [*Livina et al.*, 2011]. Our analysis suggests that after 30 ka, the climate system bifurcated from a bistable to a monostable state, as the duration and subsequent expression of D-O events reduced and then disappeared in the Greenland record (Figure 2 and Movie S1 in the supporting information). The system then returned to a bistable state during the Bølling-Allerød warming and Younger Dryas stadial (Greenland Interstadial 1 and Greenland Stadial 1, respectively) (Figures S3 and S4 in the supporting information) [*Lowe et al.*, 2008]. Importantly, the underlying potential became highly asymmetric as the system gradually lost stability around 30 ka (as shown in Figure 2). This suggests that D-O events 2–4 occurred when there was no stable interstadial state and the system was destined to return to the stadial state. It is important to note, however, that since our analysis uses a sliding window, it is difficult to identify precisely the point at which the interstadial state completely lost stability. It is therefore possible that D-O events 3 and 4 were represented by a "degenerate potential" [*Livina et al.*, 2010, 2011], a quasi-stable state close to a bifurcation.

We searched for early warning signals of this transition from a bistable to monostable state in both GICC05 and GICC05-CB by measuring the trends in autocorrelation and variance over a sliding window, both of which

are expected to increase as a bifurcation is approached due to the gradual reduction in recovery rates to perturbations (Text S1 in the supporting information) [*Dakos et al*., 2008; *Lenton et al*., 2012]. Here we observe a positive trend in autocorrelation and variance in both records approximately 10 kyr before the switch in periodicities at around 30 ka (Figure 3), consistent with the climate system experiencing a long-term forcing prior to reaching a critical threshold [*Livina et al*., 2010]. We measure the statistical evidence of the trend from the 65°N minima in summer insolation at 40 ka, and test against a null model based on randomizations of the original time series (Text S1 in the supporting information and Figure 4). Both records showed strong increasing trends in variance (Kendall $\tau > 0.8$), with type I error (p) < 0.05, and increasing trends in autocorrelation (Kendall $\tau > 0.73$), with $p < 0.05$ for GICC05 and <0.01 for GICC05-CB. Importantly, these trends reverse after 30 ka (Figure S7 in the supporting information). Finding the same trends in GICC05 and GICC05-CB in both the stability and tipping point analyses suggests that evidence for this bifurcation around 30 ka is robust regardless of the chronology used.

4.1. Mechanisms of Change: Sea Ice and Obliquity

The trends in autocorrelation and variance in both records, and resultant timing of the climate shift, parallel the decrease in the Earth's axial tilt (obliquity) [*Berger*, 1978] (Figure 1), in marked contrast to summer insolation at 65°N, which rises and then falls over the same period. Low obliquity is known to drive high sea ice extent in the Arctic due to decreased seasonality [*Mantsis et al*., 2011; *Tuenter et al*., 2005]. Sea ice extent in the Labrador Sea plays an important role in global atmospheric and ocean circulation, being associated with large surface heat flux anomalies and changes in the location and strength of the midlatitude jet stream [*Alexander et al*., 2004] (including associated snowfall δ^{18}O over Greenland) [*Hurrell*, 1995; *Kvamstø et al*., 2004; *Strong and Magnusdottir*, 2010] while also influencing North Atlantic Deep Water formation [*Rhein et al*., 2002] and Atlantic meridional overturning [*Vettoretti and Peltier*, 2013].

Given the shift to a monostable state by 30 ka was accompanied by a positive trend in autocorrelation and variance, we constructed a series of global climate simulations to test the impact of changing obliquity on the Northern Hemisphere using the Commonwealth Scientific and Industrial Research Organisation Mk3L Earth system model [*Phipps et al*., 2011] (Text S3 in the supporting information). This Earth system model has fully interactive ocean, atmosphere, land, and sea ice submodels and is designed for millennial-scale climate simulations with an ocean model resolution of 1.6° latitude × 2.8° longitude × 21 vertical levels, and an atmospheric model resolution of 3.2° latitude × 5.6° longitude × 18 pressure levels. We used four experiments in our study (Table S2 in the supporting information), with greenhouse gas and orbital forcing specified according to four periods: (i) a preindustrial control run equivalent to the year Common Era (C.E.) 1780, (ii) a 21 ka Last Glacial Maximum run, (iii) a 28.5 ka obliquity -minimum run, and (iv) a 49 ka obliquity -maximum run. We found that preindustrial sea ice extent approximately agreed with modern (C.E. 1980–1999) [*Cavalieri et al*., 1996] spatial and seasonal trends in the Labrador Sea and North Pacific (Figure S8 in the supporting information), providing confidence in the reconstructions. We initiated each experiment from a modern-day climatology and ran it for 2000 years using the forcing described in Table S2 in the supporting information. We derived the orbital parameters for the 49, 28.5, and 21 ka experiments using the Berger algorithm [*Berger*, 1978]. For greenhouse gas concentrations, we took the values reported from the Antarctic ice cores European Project for Ice Coring in Antarctica Dronning Maud Land and Dome C (Table S2 in the supporting information).

Our simulations suggest more extensive sea ice cover in the Labrador Sea and North Pacific during the minimum in obliquity (centered on 28.5 ka) relative to its peak (at 49 ka) (Figure 5). It is also important to note that the equivalent greenhouse gas radiative forcing difference was only 0.098 W m^{-2} between the maximum and minimum obliquity periods, whereas it was almost 5 times greater (0.49 W m^{-2}) between the minimum obliquity period and the LGM (Table S2 in the supporting information); while relatively small, it is probable that greenhouse gas forcing during obliquity periods still played an important secondary role in the expansion of sea ice across this period. Our simulations suggest that greatly extended sea ice cover in the Labrador Sea enhanced westerly airflow to the south of Greenland (Figure 5 and Figure S10 in the supporting information) and North Atlantic Deep Water formation was reduced substantially relative to peak obliquity at 49 ka (Figure S11 in the supporting information). With a reduction in North Atlantic Deep Water formation, the North Atlantic became cooler and fresher (Figure S10 in the supporting information), driving more extensive sea ice cover in the Labrador Sea. The North Atlantic Deep Water cell is reduced by 10% from 49 ka to 28.5 ka, compared with a 4% increase from 28.5 to 21 ka (Figure S11 in the supporting information); and the

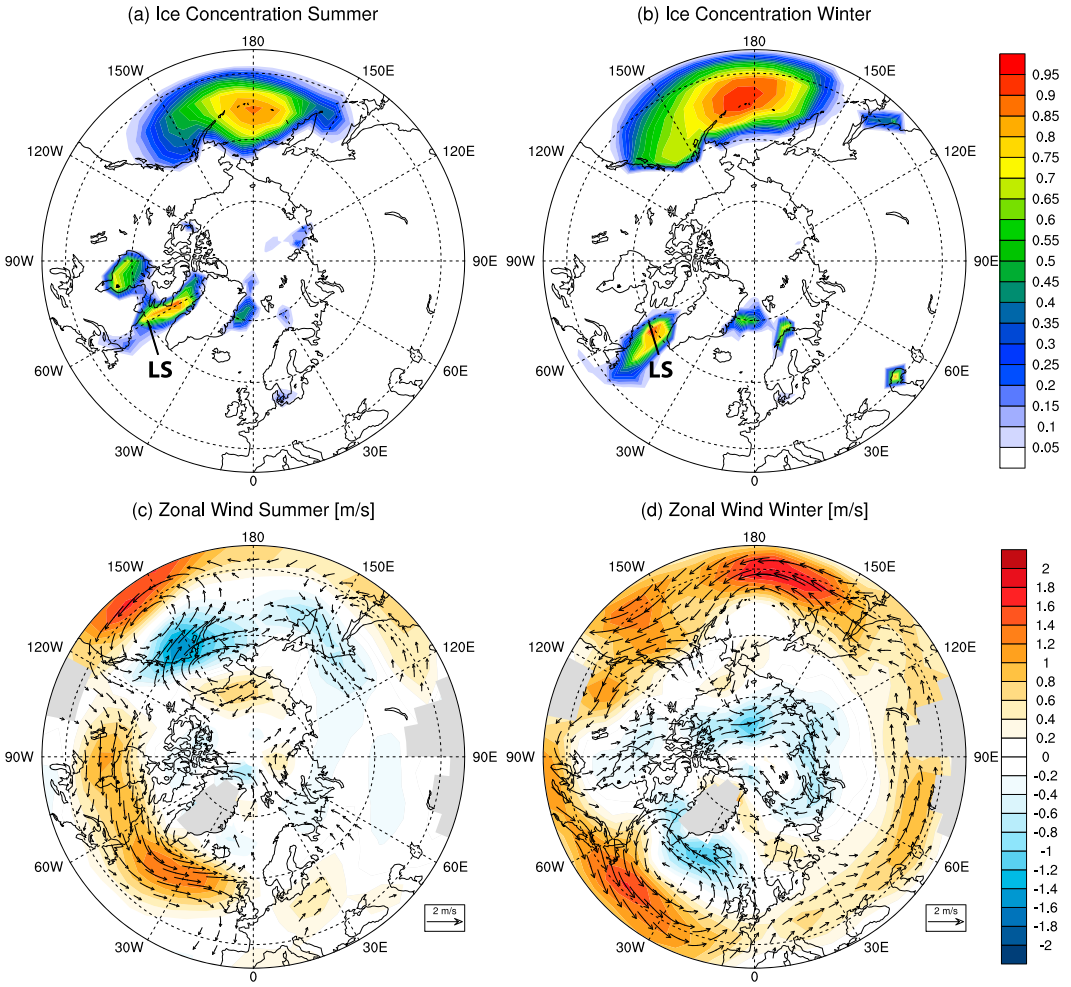

Figure 5. Modeled differences between 28.5 and 49 ka global climate model experiments showing (a and b) sea ice concentration and (c and d) zonal wind at 850 hPa (wind vectors shown; minimum threshold mask of 0.4 m s^{-1}). The (left) summer plots are average of August to October. The (right) winter plots are average of February to April, reflecting the lag in sea ice coverage behind the minimum and maximum seasonal insolation. "LS" denotes Labrador Sea.

approximate depth of the North Atlantic Deep Water cell also reduced from 2500 m at 49 ka to 1500 m at 28.5 and 21 ka. Although atmospheric changes have been shown to exert a strong influence over sea ice extent in the Labrador Sea on monthly to interannual time scales [*Deser et al.*, 2000; *Strong and Magnusdottir*, 2010], modeled simulations suggest that more extensive sea ice in the Labrador Sea might act as a negative feedback mechanism that attenuates atmospheric variation on longer (centennial) time scales [*Kvamstø et al.*, 2004], consistent with the 10 kyr parallel trends in autocorrelation, variance, and obliquity. With summer insolation at 65°N decreasing until 21 ka, our simulations show a further expansion in sea ice in the Labrador Sea, while the extensive coverage in the North Pacific was maintained (Figure S9 in the supporting information). Most importantly, our results suggest that the obliquity minimum led to a strengthening and equatorward shift in the westerly wind belt in the northwest Atlantic (Figure 5 and Figure S10 in the supporting information), reducing the delivery of air masses and expression of millennial-scale events in Greenland between 30 and 14.6 ka.

4.2. Wider Implications

The inferred increase in sea ice in the Northern Hemisphere by 30 ka coincides with reconstructions of abrupt, early cooling of deep North Atlantic waters, and reduced meridional overturning circulation [*Waelbroeck et al.*, 2002]. These changes preceded maximum continental ice volume [*Clark et al.*, 2009] and in combination with an enhanced latitudinal insolation gradient at this time [*Davis and Brewer*, 2009; *Raymo and Nisancioglu*, 2003], seem likely to have contributed to the onset of glacial conditions in the North Atlantic, with global

implications. For instance, the timing of the above state shift is identical to trends in middle- to high-latitude climate and glaciation in the Southern Hemisphere [*Fogwill et al*., 2015; *Heusser et al*., 1999; *Vandergoes et al*., 2005], suggesting synchronous global change. With the recent description of a southern high-latitude source for the interstadial warming during the Bølling-Allerød (GI-1) [*Thiagarajan et al*., 2014], we speculate that D-O events prior to 30 ka might have originated in the Southern Hemisphere [*Thomas et al*., 2011] and were only expressed in Greenland when sea ice was limited due to relatively high axial tilt, something not possible with the buffer of more extensive cover in the Labrador Sea after 30 ka. Importantly, there is evidence of reduced expression of D-O events during the previous obliquity minima (70 ka) [*North Greenland Ice Core Project Members*, 2004]. Regardless of the origin of D-O events, however, our results suggest that obliquity tipped the North Atlantic into a more frozen state, driving synchronous hemispheric climate change that led to the establishment of the Last Glacial Maximum.

Acknowledgments

This work was supported by the Australian Research Council. Numerical simulations were run on the National Computational Infrastructure National Facility at the Australian National University. Steven Phipps kindly assisted with the setup of the model simulations. The GICCO5-CB $\delta^{18}O$ record is lodged on the Paleoclimatology Database (National Oceanic and Atmospheric Administration data set ID: noaa-icecore-19015).

References

Alexander, M. A., U. S. Bhatt, J. E. Walsh, M. S. Timlin, J. S. Miller, and J. D. Scott (2004), The atmospheric response to realistic Arctic sea ice anomalies in an AGCM during winter, *J. Clim.*, *17*(5), 890–905.

Berger, A. (1978), Long-term variations of daily insolation and Quaternary climatic change, *J. Atmos. Sci.*, *35*, 2362–2367.

Bond, G., W. Broecker, S. Johnsen, J. McManus, L. Labeyrie, J. Jouzel, and G. Bonani (1993), Correlations between climate records from north Atlantic sediments and Greenland ice, *Nature*, *365*, 143–147.

Buizert, C., et al. (2015), The WAIS Divide deep ice core WD2014 chronology; Part 1: Methane synchronization (68–31 ka BP) and the gas age–ice age difference, *Clim. Past*, *11*(2), 153–173.

Cavalieri, D. J., C. L. Parkinson, P. Gloersen, and H. Zwally (1996), *Sea Ice Concentrations From Nimbus-7 SMMR and DMSP SSM/I-SSMIS Passive Microwave Data: 1980-1999 Monthly Data*, NASA DAAC at the Natl. Snow and Ice Data Cent., Boulder, Colo.

Clark, P. U., A. S. Dyke, J. D. Shakun, A. E. Carlson, J. Clark, B. Wohlfarth, J. X. Mitrovica, S. W. Hostetler, and A. M. McCabe (2009), The Last Glacial Maximum, *Science*, *325*, 710–714.

Cooper, A., C. Turney, K. A. Hughen, B. W. Brook, H. G. McDonald, and C. J. A. Bradshaw (2015), Abrupt warming events drove Late Pleistocene Holarctic megafaunal turnover, *Science*, *349*(6248), 602–606.

Dakos, V., M. Scheffer, E. H. van Nes, V. Brovkin, V. Petoukhov, and H. Held (2008), Slowing down as an early warning signal for abrupt climate change, *Proc. Natl. Acad. Sci. U.S.A.*, *105*(38), 14,308–14,312.

Davis, B. S., and S. Brewer (2009), Orbital forcing and role of the latitudinal insolation/temperature gradient, *Clim. Dyn.*, *32*(2–3), 143–165.

Deplazes, G., et al. (2013), Links between tropical rainfall and North Atlantic climate during the last glacial period, *Nat. Geosci.*, *6*(3), 213–217.

Deser, C., J. E. Walsh, and M. S. Timlin (2000), Arctic sea ice variability in the context of recent atmospheric circulation trends, *J. Clim.*, *13*(3), 617–633.

Ditlevsen, P. D., and S. J. Johnsen (2010), Tipping points: Early warning and wishful thinking, *Geophys. Res. Lett.*, *37*, L19703, doi:10.1029/2010GL044486.

Ditlevsen, P. D., K. K. Andersen, and A. Svensson (2007), The DO-climate events are probably noise induced: Statistical investigation of the claimed 1470 years cycle, *Clim. Past*, *3*(1), 129–134.

EPICA Community Members (2006), One-to-one coupling of glacial climate variability in Greenland and Antarctica, *Nature*, *444*, 195–198.

Fogwill, C. J., C. S. M. Turney, D. K. Hutchinson, A. S. Taschetto, and M. H. England (2015), Obliquity control on Southern Hemisphere climate during the Last Glacial, *Nat. Sci. Rep.*, *5*, 11673, doi:10.1038/srep11673.

He, F., J. D. Shakun, P. U. Clark, A. E. Carlson, Z. Liu, B. L. Otto-Bliesner, and J. E. Kutzbach (2013), Northern Hemisphere forcing of Southern Hemisphere climate during the last deglaciation, *Nature*, *494*(7435), 81–85.

Heusser, C. J., L. E. Heusser, and T. V. Lowell (1999), Paleoecology of the southern Chilean Lake District-Isla Grande de Chiloé During middle-late Llanquihue glaciation and deglaciation, *Geogr. Ann. Series A, Phys. Geogr.*, *81*(2), 231–284.

Hughen, K. A., J. T. Overpeck, L. C. Peterson, and S. Trumbore (1996), Rapid climate changes in the tropical Atlantic region during the last deglaciation, *Nature*, *380*, 51–54.

Hughen, K. A., J. Southon, S. Lehman, C. Bertrand, and J. Turnbull (2006), Marine-derived ^{14}C calibration and activity record for the past 50,000 years updated from the Cariaco Basin, *Quat. Sci. Rev.*, *25*, 3216–3227.

Hurrell, J. W. (1995), Decadal trends in the North Atlantic Oscillation: Regional temperatures and precipitation, *Science*, *269*, 676–679.

Ives, A. R. (1995), Measuring resilience in stochastic systems, *Ecol. Monogr.*, *65*(2), 217–233.

Kendall, M. G. (1948), *Rank Correlation Methods*, Griffen, Oxford.

Kvamstø, N. G., P. Skeie, and D. B. Stephenson (2004), Impact of Labrador sea ice extent on the North Atlantic oscillation, *Int. J. Climatol.*, *24*(5), 603–612.

Lenton, T. M., V. N. Livina, V. Dakos, E. H. van Nes, and M. Scheffer (2012), Early warning of climate tipping points from critical slowing down: Comparing methods to improve robustness, *Philos. Trans. R. Soc., A*, *370*(1962), 1185–1204.

Livina, V. N., F. Kwasniok, and T. M. Lenton (2010), Potential analysis reveals changing number of climate states during the last 60 kyr, *Clim. Past*, *6*(1), 77–82.

Livina, V. N., F. Kwasniok, G. Lohmann, J. W. Kantelhardt, and T. M. Lenton (2011), Changing climate states and stability: From Pliocene to present, *Clim. Dyn.*, *37*(11-12), 2437–2453.

Lowe, J. J., S. O. Rasmussen, S. Björck, W. Z. Hoek, J. P. Steffensen, M. J. C. Walker, Z. C. Yu, and INTIMATE Members (2008), Synchronization of paleoenvironmental events in the North Atlantic region during the Last Termination: A revised protocol recommended by the INTIMATE group, *Quat. Sci. Rev.*, *27*, 6–17.

Mantsis, D. F., A. C. Clement, A. J. Broccoli, and M. P. Erb (2011), Climate feedback in response to changes in obliquity, *J. Clim.*, *24*(11), 2830–2845.

Maslin, M. A., and C. M. Brierley (2015), The role of orbital forcing in the early middle Pleistocene transition, *Quat. Int.*, doi:10.1016/j.quaint.2015.1001.1047, in press.

Masson-Delmotte, V., J. Jouzel, A. Landais, M. Stievenard, S. J. Johnsen, J. W. C. White, M. Werner, A. Sveinbjornsdottir, and K. Fuhrer (2005), GRIP deuterium excess reveals rapid and orbital-scale changes in Greenland moisture origin, *Science*, *309*, 118–121.

Mix, A. C., E. Bard, and R. Schneider (2001), Environmental processes of the ice age: Land, oceans, glaciers (EPILOG), *Quat. Sci. Rev.*, *20*, 627–657.
North Greenland Ice Core Project Members (2004), High-resolution record of Northern Hemisphere climate extending into the last interglacial period, *Nature*, *431*, 147–151.
Overpeck, J. T., L. C. Peterson, N. Kipp, J. Imbrie, and D. Rind (1989), Climate change in the circum-North Atlantic region during the last deglaciation, *Nature*, *338*(6216), 553–557.
Paillard, D. (1998), The timing of Pleistocene glaciations from a simple multiple-state climate model, *Nature*, *391*(6665), 378–381.
Peterson, L. C., G. H. Haug, K. A. Hughen, and U. Röhl (2000), Rapid changes in the hydrologic cycle of the tropical Atlantic during the Last Glacial, *Science*, *290*, 1947–1951.
Phipps, S. J., L. D. Rotstayn, H. B. Gordon, J. L. Roberts, A. C. Hirst, and W. F. Budd (2011), The CSIRO Mk3L climate system model version 1.0 – Part 1: Description and evaluation, *Geosci. Model Dev.*, *4*(2), 483–509.
Rasmussen, S. O., et al. (2014), A stratigraphic framework for abrupt climatic changes during the Last Glacial period based on three synchronized Greenland ice core records: Refining and extending the INTIMATE event stratigraphy, *Quat. Sci. Rev.*, *106*, 14–28.
Raymo, M. E., and K. H. Nisancioglu (2003), The 41 kyr world: Milankovitch's other unsolved mystery, *Paleoceanography*, *18*(1), 1011, doi:10.1029/2002PA000791.
Rhein, M., J. Fischer, W. M. Smethie, D. Smythe-Wright, R. F. Weiss, C. Mertens, D. H. Min, U. Fleischmann, and A. Putzka (2002), Labrador sea water: Pathways, CFC inventory, and formation rates, *J. Phys. Oceanogr.*, *32*(2), 648–665.
Rind, D. (1998), Latitudinal temperature gradients and climate change, *J. Geophys. Res.*, *103*, 5943–5971.
Rind, D., M. Chandler, J. Lerner, D. G. Martinson, and X. Yuan (2001), Climate response to basin-specific changes in latitudinal temperature gradients and implications for sea ice variability, *J. Geophys. Res.*, *106*(D17), 20,161–20,173.
Schulz, M. (2002), On the 1470-year pacing of Dansgaard-Oeschger warm events, *Paleoceanography*, *17*(2), 1014, doi:10.1029/2000PA000571.
Strong, C., and G. Magnusdottir (2010), Modeled winter sea ice variability and the North Atlantic Oscillation: A multicentury perspective, *Clim. Dyn.*, *34*(4), 515–525.
Svensson, A., et al. (2008), A 60 000 year Greenland stratigraphic ice core chronology, *Clim. Past*, *4*, 47–57.
Theiler, J., S. Eubank, A. Longtin, B. Galdrikian, and J. Doyne Farmer (1992), Testing for nonlinearity in time series: The method of surrogate data, *Phys. D: Nonlinear Phenom.*, *58*(1–4), 77–94.
Thiagarajan, N., A. V. Subhas, J. R. Southon, J. M. Eiler, and J. F. Adkins (2014), Abrupt pre-Bolling-Allerod warming and circulation changes in the deep ocean, *Nature*, *511*(7507), 75–78.
Thomas, A. M., S. Rupper, and W. F. Christensen (2011), Characterizing the statistical properties and interhemispheric distribution of Dansgaard-Oeschger events, *J. Geophys. Res.*, *116*, D03103, doi:10.1029/2010JD014834.
Timmermann, A., H. Gildor, M. Schulz, and E. Tziperman (2003), Coherent resonant millennial-scale climate oscillations triggered by massive meltwater pulses, *J. Clim.*, *16*, 2569–2585.
Tuenter, E., S. L. Weber, F. J. Hilgen, and L. J. Lourens (2005), Sea-ice feedback on the climatic response to precession and obliquity forcing, *Geophys. Res. Lett.*, *32*, L24704, doi:10.1029/2005GL024122.
Tzedakis, P. C., K. Hughen, I. Cacho, and K. Harvati (2007), Placing late Neanderthals in a climatic context, *Nature*, *449*, 206–208.
van Nes, E. H., and M. Scheffer (2007), Slow recovery from perturbations as a generic indicator of a nearby catastrophic shift, *Am. Nat.*, *169*(6), 738–747.
Vandergoes, M. J., R. M. Newnham, F. Preusser, C. H. Hendy, T. V. Lowell, S. J. Fitzsimons, A. G. Hogg, H. U. Kasper, and C. Schluchter (2005), Regional insolation forcing of late Quaternary climate change in the Southern Hemisphere, *Nature*, *436*(7048), 242–245.
Vettoretti, G., and W. R. Peltier (2013), Last Glacial Maximum ice sheet impacts on North Atlantic climate variability: The importance of the sea ice lid, *Geophys. Res. Lett.*, *40*, 6378–6383, doi:10.1002/2013GL058486.
Waelbroeck, C., L. Labeyrie, E. Michel, J. C. Duplessy, J. F. McManus, K. Lambeck, E. Balbon, and M. Labracherie (2002), Sea-level and deepwater temperature changes derived from benthic foraminifera isotopic records, *Quat. Sci. Rev.*, *21*(1–3), 295–305.
WAIS Divide Project Members (2015), Precise interpolar phasing of abrupt climate change during the last ice age, *Nature*, *520*(7549), 661–665.
Wolff, E. W., J. Chappellaz, T. Blunier, S. O. Rasmussen, and A. Svensson (2010), Millennial-scale variability during the last glacial: The ice core record, *Quat. Sci. Rev.*, *29*(21-22), 2828–2838.
Wunsch, C. (2003), Greenland—Antarctic phase relations and millennial time scale climate fluctuations in the Greenland ice cores, *Quat. Sci. Rev.*, *22*(15–17), 1631–1646.